Supporting Information

Details of experimental methods, supplementary figures, additional results and discussion, table of mass-to-charge values.

Supporting Figures and Tables are provided below the Supporting information sections (after section S13).

Bioactivity Profiling of Small-Volume Samples by Nano Liquid Chromatography Coupled to Microarray Bioassaying Using High-Resolution Fractionation

Barbara M. Zietek,[†,○] Kristina B. M. Still,[†,○] Kevin Jaschusch,[†] Ben Bruyneel,[†] Freek Ariese,[‖] Tinco J. F. Brouwer,[‡] Matthijs Luger,[‡] Rob J. Limburg,[‡] Joost C. Rosier,[§] Dick J. v. Iperen,[§] Nicholas R. Casewell,[⊥,#] Govert W. Somsen,[†] and Jeroen Kool[*,†]

† Division of BioAnalytical Chemistry, Amsterdam Institute of Molecules, Medicines and Systems, Vrije Universiteit Amsterdam, Amsterdam 1081 HZ, The Netherlands

‡ Electronic Engineering, Vrije Universiteit Amsterdam, Amsterdam 1081 HV, The Netherlands

§ Fine Mechanics and Engineering Beta-VU, Vrije Universiteit Amsterdam, Amsterdam 1081 HV, The Netherlands

‖ LaserLaB, Vrije Universiteit Amsterdam, Amsterdam 1081 HV, The Netherlands

⊥Centre for Snakebite Research & Interventions, Liverpool School of Tropical Medicine, Pembroke Place, Liverpool L3 5QA, U.K.

Centre for Drugs and Diagnostics, Liverpool School of Tropical Medicine, Pembroke Place, Liverpool L3 5QA, U.K.

*E-mail: j.kool@vu.nl.

Author Contributions

○ B.M.Z. and K.B.M.S. contributed equally.

S1. Chemicals

Monobasic- and dibasic- trihydrate potassium phosphate, Trizma base, glycerol, acetone, methyltrimetoxysilane (MTMOS), leupeptin hemisulphate salt microbial ≥90% (HPLC), aprotinin, mineral oil (light oil, for molecular biology), bovine serum albumin (BSA) and 7-amino-4-methylcoumarin were all from Sigma-Aldrich (Zwijndrecht, The Netherlands). Sulfuric acid was from Merck (Darmstadt, Germany), hydrochloric acid and dimethyl sulfoxide (DMSO) were from Riedel-de-Haën (Zwijndrecht, The Netherlands). Human plasmin was from Haematologic Technologies, Inc. (Essex, Junction, VT, USA) and was used at a stock concentration of 0.435 mg/mL in glycerol:water (1:1, v/v). H-D-Val-Leu-Lys-AMC acetate salt from Bachem (Bubendorf, Zwitserland) was used at a stock concentration of 20 mM in DMSO. Leupeptin hydrochloride and aprotinin were dissolved in MilliQ water to their stock concentrations of 10 mM and 1 mg/ml, respectively. Acetonitrile MS grade, methanol, formic acid and trifluoroacetic acid were all from Biosolve (Valkenswaard, The Netherlands). MilliQ water was obtained from a direct-QTM Millipore system Millipore (Millipore, Billerica, MA, U.S.)

S2. Preparation and Coating of Glass Slide with MTMOS

Prior to coating with methyl trimethoxylsilane (MTMOS) solution, glass slides were washed with milliQ water. Clean glass slides were then placed on a removable glass slide rack and dried under a stream of compressed air (CA). The dried glass slides were then immersed in concentrated sulfuric acid (98%) overnight (O/N). The sulfuric acid was subsequently removed by rinsing the glass slides thoroughly with water, by first rinsing the glass slides with fresh water for minimum of 15 min. To remove water the acid free glass slides were then submerged for a few seconds in acetone, after which the slides were dried under CA. The resulting acid cleaned glass slides were stored dry in the dark prior to coating.

The hydrophobic mixture used for coating comprised 8 mL of 95% MTMOS liquid, 3.2 mL of 5 mM HCl in water, and 8 mL of KPO_4 buffer (25 mM) at pH 8. This mixture was prepared by first mixing 8 mL MTMOS solution with 3.2 mL of 5 mM HCl using a vortex mixer at 2200 rpm for 2 min in a 50 mL Greiner tube. The mixture was then placed in an ultrasonic water bath (Bransonic, Valkenswaard, The Netherlands) for 15 min. After ultra-sonication, 8 mL of KPO_4 buffer (25 mM) at pH 8 was added to the emulsion and briefly shaken.

The coating of the acid-cleaned glass slides was performed by 1) placing a glass slide into an in-house made glass slide holder of the in-house made spin coater (made of a modified Maxtor 90650U2 hard drive with a switching power supply); 2) covering the spin coater with a transparent lid with a hole in the center; 3) dispensing 4 mL of the freshly prepared coating mixture using a 5 mL pipette over a

spinning acid-cleaned glass slide through the hole in the center of the transparent cover. The spin coater was operated at a fixed spinning speed of 5400 rpm for 30 s. Details and photos of the spin coater can be found in Figure S1.

S3. NanoLC Gradient

The gradient used for leupeptin and aprotinin started at 2% B for 6 min and then linearly increased to 60% B in 20 min and then to 90% B in the next 5 min. After an additional 3 min elution at 90% B, the column was reequilibrated at starting conditions (2% B) for 7 min. The total analysis time was 35 min. For the analysis of a mixture of leupeptin diastereoisomers (25 µM leupeptin) and snake venom samples the gradient was from 1% B to 60% B in 36 min and then in 2 min to 90% B, where it stayed isocratic for 2 min. At 44.1 min, mobile phase B decreased to 1% (starting conditions) and continued at this concentration until 60 min. The nanoLC system was controlled by Chromeleon version 6.80 SR12 software. For MS analysis, the samples were rerun using the same gradient. For MS analysis, leupeptin diastereoisomers were separated at a leupeptin concentration of 2 µM.

S4. Preparation of a Capillary Used for Effluent Picofractionation

For the picofractionation, ~30 cm of a fused-silica capillary of 75 µm I.D. and 365 µm O.D. was used of which the blunt tip was coated on the outside with MTMOS. Prior to coating with MTMOS solution, one end of the capillary was closed - by melting it with a burner - to prevent blocking the inside of the capillary with MTMOS solution during the coating process. The heating of the capillary was also done to remove the polyamide coating (3-4 cm of the tip). Coating with MTMOS solution (silylation) of the capillary tip was performed by immersing ~4 cm of the capillary (at this point closed) tip into MTMOS coating solution for ~5 min, after which the capillary was dried at ambient atmosphere (O/N placed in a fume-hood). The MTMOS coated tip was opened with the use of a capillary cutter in a straight line prior to use.

S5. Image Acquisition and Processing of The Microarray Data

Fluorescence intensities of the microarray bioassay droplets were measured kinetically by taking 24-bit images of 1200 pixels x 1200 pixels (width and height, respectively) separately for each bioassay droplet during incubation (i.e. developing microarray bioassay droplets). The time to acquire images of a complete microarray bioassay containing up to 300 single bioassay reactions was 7.5 min. In µManager, the Lumascope LED C, Channel C was selected with LED C illumination set to 160, camera gain set to 15, and camera image mode at RGB32. The multi-dimensional acquisition (MDA) option available in µManager enabled acquisition at multiple stage positions, in a serpentine fashion to follow the picofractionation pattern. The camera exposure time was set at 300 ms. Kinetic

measurements were performed by taking 18 images of every single bioassay droplet reaction in intervals of 7.5 min. Captured images were saved as separate image files for further processing.

Fluorescence intensity for images with single spots at all intervals was calculated with the following equation[1]: Net Total Fluorescence Intensity = Integrated Density – (area of an image × fluorescence intensity of the background mean), using ImageJ[2]. In the equation, the Integrated Density of an image is the intensity of an entire image (containing the background and the fluorescence spot over an area of 1200 pixels x 1200 pixels). The mean fluorescence background intensity – for a complete microarray bioassay experiment – was measured using 20 randomly picked images acquired during the first interval of the measurement. In each of the 20 images, an area outside of the droplet was selected and the background intensity was extrapolated to get the background for a 1200 x 1200 pixel area. In order to automate processing of the acquired images and construct bioactivity chromatograms, an in-house written macro was implemented in ImageJ. Subsequently, a script written in R[3] was used to generate a kinetic curve for each microarray bioassay spot from each time interval measured using the calculated net total fluorescence intensity. The same R script was used to calculate slopes from the kinetic curves for each bioassay droplet reaction, which were finally plotted against their picofractionation time to create microarray bioactivity chromatograms (MBCs). The macro used for processing the data to obtain the MBCs can be found in Supporting Information S12.

S6. Performance of The Plasmin Microarray Bioassay

The performance of the microarray bioassay was first evaluated by determining IC50 values of the two plasmin inhibitors leupeptin and aprotinin. Leupeptin was analyzed at ten different concentrations ranging from 0-400 µM, and aprotinin at nine different concentrations ranging from 0-30 µM. The inhibitors were serially diluted in MilliQ water. To mimic nanoLC solvent delivery while still maintaining a continuous flow of the inhibitor solutions, nanoliter spots of the inhibitors were collected on MTMOS coated glass slides with the help of a syringe pump model 22 from Harvard Apparatus (Holliston, MA, USA). The inhibitors were delivered via a fused-silica capillary connected to a 250 µL volume Hamilton glass syringe (Supleco, Bellefonte, PA, USA) mounted on the syringe pump. Droplets of 100-nL formed at the tip of the capillary were dislodged/detached using 100 nL droplets ejected every 4 s with solenoid valve 1. Each inhibitor concentration to be bioassayed was spotted 5 times on two different glass slides. Next, the dried spots were exposed to the plasmin microarray bioassay following the same procedure as described earlier in the text.

S7. Quality of the plasmin microarray bioassay

In order to calculate the Z'-factor of the microarray bioassay, positive control samples (n=100) of 200 µM leupeptin (ensuring total enzyme inhibition) and negative control samples (n=100) consisting of

mobile phase A were spotted in the same manner as described for the IC50 determination. Subsequent bioassay and data processing was done following the same procedure as described in the experimental section to obtain the kinetic slopes of each microarray reaction droplet data point. Using these kinetic slopes, the Z'-factor was calculated according to Zhang et al.[4].

S8. Bioassay Droplets In Oil – Evaporation Observation

A mixture of enzyme and substrate (final concentration of enzyme was 200 ng/mL and substrate 5 µM) were deposited in a non-contact manner onto an MTMOS-coated glass slide, and directly covered by mineral oil droplet. The droplets were deposited in triplicate. 30 minutes after deposition (incubation in normal assay protocol) the droplets were monitored every 1.5 hours for 12 hours.

The results (Figure S8) show that the mineral oil droplet shape and size is not affected in time. A slight change is observed (only between the first two measurements) in the (watery) bioassay droplet mixture inside the oil. This is most likely due to the hydrophobicity of the coating on the glass slide. It is thought that, rather than droplet evaporation, the change in shape occurs due to the upward push in order to decrease its surface area contact on the hydrophobic coated glass slide. Effectively, a slight rearrangement in the oil, which appears as a decrease in droplet size. We are not able to accurately monitor the possible change in height of the droplet in oil with the current setup to confirm this.

S9. Nanofractionation of Venoms and The Standards

The bioassay in 384 well plates for the analysis of the serial dilution of leupeptin and aprotinin and analysis of crude snake venoms was performed using a Shimadzu high-performance liquid chromatography (HPLC) system ('s Hertogenbosch, The Netherlands) consisting of a Shimadzu SIL-30 AC autosampler and two Shimadzu LC-30AB pumps, which were interfaced to an Bruker MAXIS Q-TOF MS instrument (Bruker, Bremen, Germany). The snake venoms *B. asper*, *D. acutus*, *T. trigonocephalus* and *T. purpureomaculatus* were injected in a concentration of 1 mg/mL and 4 mg/mL (injected volume, 45 µL). Leupeptin and aprotinin standards (injected volume, 20 µL) were analyzed at five different concentrations (ranging from 10 to 100 µM and 0.077 µM to 30 µM, respectively). A 150 × 4.6 mm ID analytical column packed with XbridgeTM BEH300 reversed-phase C18 material (5 µm) was used for separations and was maintained at 37°C in a Shimadzu CTD-30A column oven. Gradient elution was performed employing mobile phase A (98% water, 2% ACN, 0.1% FA (v/v/v)) and mobile phase B (98% ACN, 2% water, 0.1% FA (v/v/v)). The gradient used for separation started at 0% B with a linear increase to 50% B in 20 min followed by an increase to 90% B in 2 min. The gradient was held at 90% B for 2 min, and then returned in 1 min to the starting conditions (0% B). Column reequilibration was 5 min, resulting in a total analysis time of 30 min. The flow rate was 0.5 mL/min. The column eluate was split in a 1:9 ratio using a low-dead-volume flow splitter. The

smaller flow (10%) was directed to a SPD-M30A detector and further directed to MaXis II QTOF mass spectrometer (Bruker Daltonics, Bremen, Germany), equipped with electrospray ionization source (ESI) and operated in positive ion mode. The parameters of the ESI source were as follows: source temperature, 180 C; desolvation temperature, 180 C; capillary voltage, 4500 V; gas flow, 4 L/min. The monitored mass range was m/z 50–2000 range with a data-sampling time of 1 s. The larger flow (90%) of the eluate was directed to an in-house developed nanofractionation system. Briefly, the system was built from a modified 235 Gilson autosampler, here a fused silica capillary extension connected to LC tubing made of polyether ether ketone (PEEK) was mounted to the robotic arm, allowing the capillary needle to move in xy directions. Fractions of 6 s were collected onto a black 384- well plate (Greiner Bio One, Alphen aan den Rijn, The Netherlands) in a serpentine fashion. After nanofractionation, the plates were evaporated overnight (O/N) using a RVC 2–33 CD plus maxi concentrator (Salm en Kipp, Breukelen, The Netherlands) with a rotation speed of 1500 rpm, pressure of 0.10 mbar, and temperature of 30 °C. After solvent evaporation, the dried plates were stored at − 20 °C prior to bioassaying.

The plasmin assay for activity screening was performed as in Zietek et al.[5]. Briefly, the bio-assay mixture was prepared by carefully mixing equal volumes of substrate (final concentration 5 μM fluorogenic substrate H-D-Val-Leu-Lys-AMC) and the enzyme (final concentration 100 ng/mL plasmin) solutions in 100 mM Tris-HCl buffer (pH 7.5) with 0.1% BSA (w/v). Directly after preparing, 50 μL of the bioassay mixture was pipetted over a black 384-well plate (Greiner Bio One, Alphen aan den Rijn, The Netherlands) using a Multidrop 384 reagent dispenser (Thermo Scientific, Ermelo, The Netherlands) or 200 μL multichannel pipet. A VarioSkan LUX microplate multimode reader (Thermo Scientific, Ermelo, The Netherlands) was used to measure fluorescence of each well kinetically at 380 and 460 nm excitation and emission wavelength, respectively. The temperature inside the plate reader was set at 37 °C. Each measurement comprised 30 cycles allowing generation of a kinetic curve. The slope of each kinetic curve was plotted against the time of nanofraction collection, producing a reconstructed bioassay chromatogram. Negative peaks in the bioactivity trace represent inhibition of plasmin, and positive peaks indicate the presence of plasmin inducers or, more likely in the case of venoms, proteases exhibiting an enzymatic activity similar to plasmin.

For comparison of the performance of the picofractionation analytics with nanofractionation analytics, the same four venoms were nanofractionated at concentrations of 1 mg/mL and 4 mg/mL (data of the 1 mg/ml venoms are not shown as for none of these analyses, any positive or negative bioassay signal was observed) under the same conditions as described by Zietek et al.[5] In Figure S9, it is shown that only *Bothrops asper* showed bioactivity signals at a concentration of 4 mg/mL, and the results obtained were similar to the picofractionation results. All the other snakes showed no visible activity (Figure S10). Although, in the results obtained using the picofractionation platform the other three venoms, i.e. *Deinagkistrodon acutus*, *Trimeresurus trigonocephalus* and *Trimeresurus*

purpureomaculatus showed bioactivity signals in a concentration of 1 mg/mL (Figure 5 and Figure S6), it has to be noted that the bioactive signals for these analyses were low. Due to sample pre-concentration on the nanoLC column after injection, the eluting sample components in picofractionation analytics are much higher than for nanofractionation. Therefore, its apparent sensitivity for these analyses is higher and as such only for picofractionation for all four snakes analyzed bioactivity signals were observed (for the highest possible concentration injected of 4 mg/mL). For nanofractionation, the detection limit was thus not sufficient to successfully analyze *Deinagkistrodon acutus*, *Trimeresurus trigonocephalus* and *Trimeresurus purpureomaculatus* for bioactivity.

In addition, also for comparison and method validation, we now analyzed the standards leupeptin and aprotinin at the same concentrations as tested for the picofractionation analytics using the nanofractionation analytics. For the standards, merging broad peaks were observed for the picofractionation analytics when injected at high concentration (due to the preconcentration of the analytes on the nanoLC column), which separated into individual sharper peaks upon injecting more diluted samples. As a consequence, lower concentrations of the standards leupeptin and aprotinin can still be observed for picofractionation as compared to nanofractionation (see Figure S11 and S12 for the results obtained by nanofractionation analytics). This clearly shows the increased sensitivity of picofractionation as compared to nanofractionation analytics and it shows that picofractionation does not give lower resolution than nanofractionation analytics, but gives overlapping peaks due to bioassay saturation upon high concentrations injected, which separate into individual baseline separated sharp peaks upon injecting more diluted samples. As a consequence, much lower concentrations of the standards leupeptin and aprotinin can still be observed for picofractionation as compared to nanofractionation (see Figure S11 and S12, and Figure 3).

S11. Picofractionation Frequency Comparison

In this research we aimed at collecting 50 nL fractions of the nanoLC effluent, which is exactly 1000 times less than in our previous research. This resulted in 10-s fractions. Fractionation frequency can have an impact on the resolution of the microarray bioactivity chromatograms. However, it will not give any improvement in our study as the chromatographic peaks of the venom toxins in our separations have much larger peak widths than the 10-s regime. The effective fraction volume when collecting 6-s fractions (as done for our nanofractionation analytics study by Zietek et al.[5]) is 30 nL. Due to the hydrophobic coating on the end of the effluent capillary, this 30 nL effluent visibly protrudes out far enough to be effectively deposited on the glass slide by contactless deposition. We have compared the difference in bioassay readout when collecting 6s fractions and 10 s fractions. For this, five spots were picofractionated onto the glass slide with both fractionation velocities. Four of these spots were exposed to the plasmin assay, for both fractionation velocities (Figure S13). As can be seen in this figure, both fractionation velocities, show very similar bioactivity curves.

In addition, these figures also demonstrate how bioactivity is screened in our picofractionation platform. Effectively, each spot on the glass slide is photographed 18 times. An increase in fluorescent readout is observed in time with positive bioassay performance. This fluorescent intensity can be determined, and with that a curve can be plotted. The slope of all these kinetic curves is used for reconstructed bioassay chromatograms. Further details of this are described in SI sections S5 and S12.

S12. An in-house written macro was implemented in ImageJ for automatic measurement of Integrated Density, Mean (Mean Grey Value), and Area of each image representing each microarray bioassay droplet reaction at each time point measurement.

```
/*
 * Local settings
 * --------------
 *
 * There are some variables you can change below.
 * some functionality needed by this script.
 *
 * roiWidth, roiHeight. default: 800, 800
 * --------------------------------------
 *
 * The width and height of the region of interest in the image.
 * The ROI is always centered in the image. The offsets are calculated
 * in ProcessImage().
 *
 *
```

```
 * checkROI, default: false
 * ------------------------
 *
 * When this variable is set to true the program will pause at each
 * image with the ROI shown.
 * You can adjust the ROI at this point before the image is analyzed.
 *
 * This option exists so you can view each image with the ROI to see
 * if it needs adjustment for the batch processing.
 *
*/

// The minimum version to use
requires("1.51r")

////////////////////////////////////////////////////////////////////////////
// Variables that are user configurable

// If this variable is set to true the program will halt at each ROI so you
// can check if the ROI is not too small or too large.
// Also BatchMode is disabled (images will be shown).
checkROI = false;

// These are needed for the ROI for each image and are used in processImage().
// You can use checkROI = true for manual inspection of each image with this
// ROI settings.
//var roiXOffset = 200; Are calculated in ProcessImage().
//var roiYOffset = 200;
var roiWidth = 800;
var roiHeight = 800;

// Print to the log window or not. Used in echo().
var printLog = true;

////////////////////////////////////////////////////////////////////////////
// Start working

// Use the date for saving the results.
dateStarted = GetDateTimeString();
echo("Starting at: " + dateStarted);

// Don't display images during batch processing
if(!checkROI)
	setBatchMode(true);

// The directory where all images are stored
// Select the directory where the images are stored.
imageDirectory = getDirectory("Choose a Directory");

// replace '\' with '/'.
imageDirectory = replace(imageDirectory, File.separator, "/");
```

```
// Get the parent path and working directory. Needed for saving the results
parentDir = File.getParent(imageDirectory);
workingDir = File.getName(imageDirectory);

// ------------------------------------------------------
// Clear previous results
run("Clear Results");

// ------------------------------------------------------
// Sort the images into order. The problem is that the folders are numbered
// without leading zeroes and just sort on ASCII.
// Also each PosN directory can contain multiple images

// Find the max PosN number
echo("Scanning: " + imageDirectory);

maxIndex = findMaxPosNumber(imageDirectory);
echo("PosN directories found = " + maxIndex);
if(maxIndex < 0)
{
	echo("No images found!");
	showMessage("<html><h1><font color=red>No images found</font></h1><font color=blue>" +
imageDirectory + "</font><html>");
	exit;
}


// ------------------------------------------------------
// Build a array with all the images

// This array holds all images and is filled by buildImageList()
var imagesAr = newArray();

// This array holds the file times
var timeAr = newArray();

buildImageList(imageDirectory);

echo("Number of images found: " + imagesAr.length);


// ------------------------------------------------------
// Now we are ready to process each image

echo("Start analyzing images");

timeZero = 0.0;

for(i = 0; i < imagesAr.length; i++)
{
```

```
        // Fetch the posN number
        start = indexOf(imagesAr[i], "/Pos");
        end  = indexOf(imagesAr[i], "/img_");
        posN = parseInt(substring(imagesAr[i], start+4, end), 10);

        // Fetch the image_N number
        start = indexOf(imagesAr[i], "/img_");
        end  = indexOf(imagesAr[i], "_Channel");
        imgN = parseInt(substring(imagesAr[i], start+5, end), 10);

//      echo("Process: " + imagesAr[i]);

        togo = imagesAr.length - i - 1;
        echo("\\Update:Images to go " + togo);

        processImage(posN, imgN, imagesAr[i]);

        // Get the file time difference in seconds
        fileTime = parseFloat(File.lastModified(imagesAr[i]));

        // Set the initial timestamp
        if(i == 0)
                timeZero = fileTime;

        // Get the differnce in seconds with the first image.
        timeDiff = (fileTime - timeZero)/1000;

        setResult("fileTime", nResults-1, timeDiff);
}


// -------------------------------------------------------
// Saving the results

file = parentDir + "/" + dateStarted + "-" + workingDir + ".csv";
//file = "M:/Projects/Lumascope/Results.csv";

echo("Saving results: " + file);
saveAs("Results", file);

echo("Finished at " + GetDateTimeString());
showMessage("<html><h1><font color=green>Ready</font></h1> " +
                      "I have analyzed <font color=blue><b>" + nResults + "</b></font> images
and saved the results at:" +
                      "<br><font color=blue><b>" + file + "</b></font></html>");

exit;


////////////////////////////////////////////////////////////////////////
// Functions
```

```
/**
 * Find the highest number in the list
 *
 * Scans the file path for '/PosN/img_' where N is the index number.
 *
 * @param directory The directory with all the PosN directories
 *
 * @return max The highest index number found or < 0 if nothing found
 */
function findMaxPosNumber( directory )
{
	max_index = -2;

	list = getFileList(imageDirectory);

	for(i=0; i<list.length; i++)
	{
		if(endsWith(list[i], "/"))
		{
			start = indexOf(list[i], "/Pos");
			end  = indexOf(list[i], "/");

			posN = parseInt(substring(list[i], start+4, end), 10);

			if(posN > max_index)
				max_index = posN;
		}
	}

	// So there at least maxIndex folders
	max_index++;

	return(max_index);
}

/**
 * Create an array with all images sorted on PosN and img_N.
 *
 * @global imagesAr The array with all images (full file path)
 */
function buildImageList( imageDirectory )
{
	// Go through each posN folder
	for(i = 0; i < maxIndex; i++)
	{
		// Create the directory path
		posDirectory = imageDirectory + "Pos" + i;

		list = getFileList(posDirectory);
```

```
                if(list.length > 0)
                {
                        ar = newArray();

                        // Find any image files
                        for(j = 0; j < list.length; j++)
                        {
                                if(endsWith(list[j], '.tif'))
                                {
                                        ar = Array.concat(ar, list[j]);
                                }
                        }

                        // Sort on the file name
                        Array.sort(ar);

                        for(j = 0; j < ar.length; j++)
                        {
                                imagesAr = Array.concat(imagesAr, posDirectory + "/" + ar[j]);
                        }
                }
        }
}


/**
 * Process each image
 *
 * In this function all the hard work is taking place for each image.
 * The results are stored in the Results table.
 *
 * @param index The index number of the image
 *
 * @param file The filename of the image
 */
function processImage( posIdx, imgIdx, file )
{
        // Open the image
        open(file);

        imageName=getTitle();

//      run("Duplicate...", "TempImage");
//      run("8-bit");

        // Create the Region Of Interest
        width = getWidth();
        height = getHeight();

        roiXOffset = (width - roiWidth) / 2;
        roiYOffset = (height - roiHeight) / 2;
```

```
        makeRectangle(roiXOffset, roiYOffset, roiWidth, roiHeight);

        if(checkROI)
                waitForUser("Is the ROI correct?");

        // Add it to the roi manager
//      roiManager("Add");

        // Open the ROI in a sepaarate window
        run("Duplicate...", "TempImage");

        // Close the original one
        close(imageName);

  // Set the measurements options
        run("Set Measurements...", "area mean integrated redirect=None decimal=1");

        // Measure it!
        run("Measure");

        // Add the pos index and image index to the Results
        setResult("posIdx", nResults-1, posIdx);
        setResult("imgIdx", nResults-1, imgIdx);
        updateResults();

        // Close the ROI image
        close();
}

/**
 * Get a datetime string
 *
 * This function returns a datetime string in the following format:
 *
 *   YYYYMMDDhhmm
 *
 * @return The datetime string
 *
 */
function GetDateTimeString()
{
        getDateAndTime(year, month, dayOfWeek, dayOfMonth, hour, minute, second, msec);

        // Months are 0 based
        month++;

        // Add a '0' prefix if needed
        monthPrefix = "";     if(month < 10)        monthPrefix = "0";
        dayPrefix  = "";      if(dayOfMonth < 10)   dayPrefix  = "0";
        hourPrefix  = "";     if(hour < 10)         hourPrefix  = "0";
```

```
	minutePrefix = "";	if(minute < 10)		minutePrefix = "0";

	date = "" + year + monthPrefix + month + dayPrefix + dayOfMonth + hourPrefix + hour +
minutePrefix + minute;

	return date;
}

/**
 * Print text to the log window
 *
 * Print only if printLog is true. because if printing the
 * log window will be opened.
 *
 * @param text Text to print
 * @global printLog true or false
 */
function echo( text )
{
	if(printLog)
		print(text);
}
```

S13. References

(1) McCloy, R. A.; Rogers, S.; Caldon, C. E.; Lorca, T.; Castro, A.; Burgess, A. *Cell Cycle* **2014**, *13* (9), 1400–1412.

(2) Rasband, W. S. ImageJ https://imagej.nih.gov/ij/.

(3) R Core Team. Vienna, Austria 2018.

(4) Zhang, J.-H.; Thomas, D. Y.; Oldenburg, K. R. *J. Biomol. Screen.* **1999**, *4* (2), 67–73.

(5) Zietek, B. M.; Mayar, M.; Slagboom, J.; Bruyneel, B.; Vonk, F. J.; Somsen, G. W.; Casewell, N. R.; Kool, J. *Anal. Bioanal. Chem.* **2018**, *410*, 5751–5763.

Supporting Figures and Tables

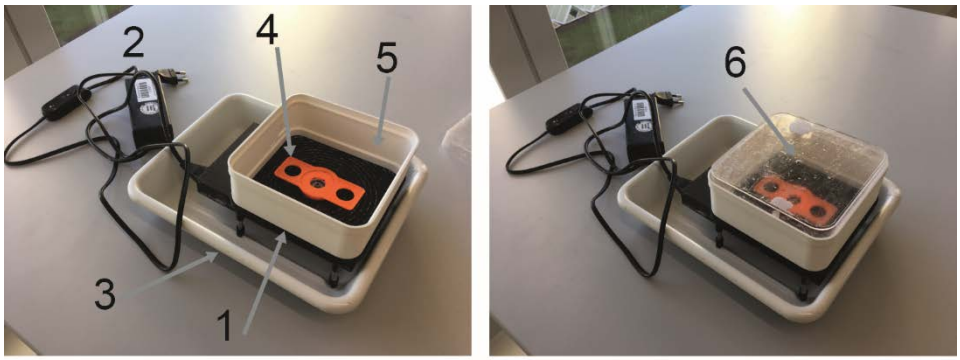

Figure S1. Spin coater made in-house from a modified Maxtor 90650U2 hard drive. 1) hard drive; 2) switching power supply; 3) drain container collecting excess of coating solution; 4) rotating holder for a glass slide; 5) box with a lid to contain the spin coater and the coating solution while spin coating. The height of the box was important as it determined the distance between the lid and the glass slide during coating. Right in figure: spin coater with the lid. Coating solution was pipetted through a small hole in the center of the plastic cover (indicated with an arrow (6)) while the glass slide was spinning. The spin coater was turned off after 30 min from the time the coating liquid was dispensed.

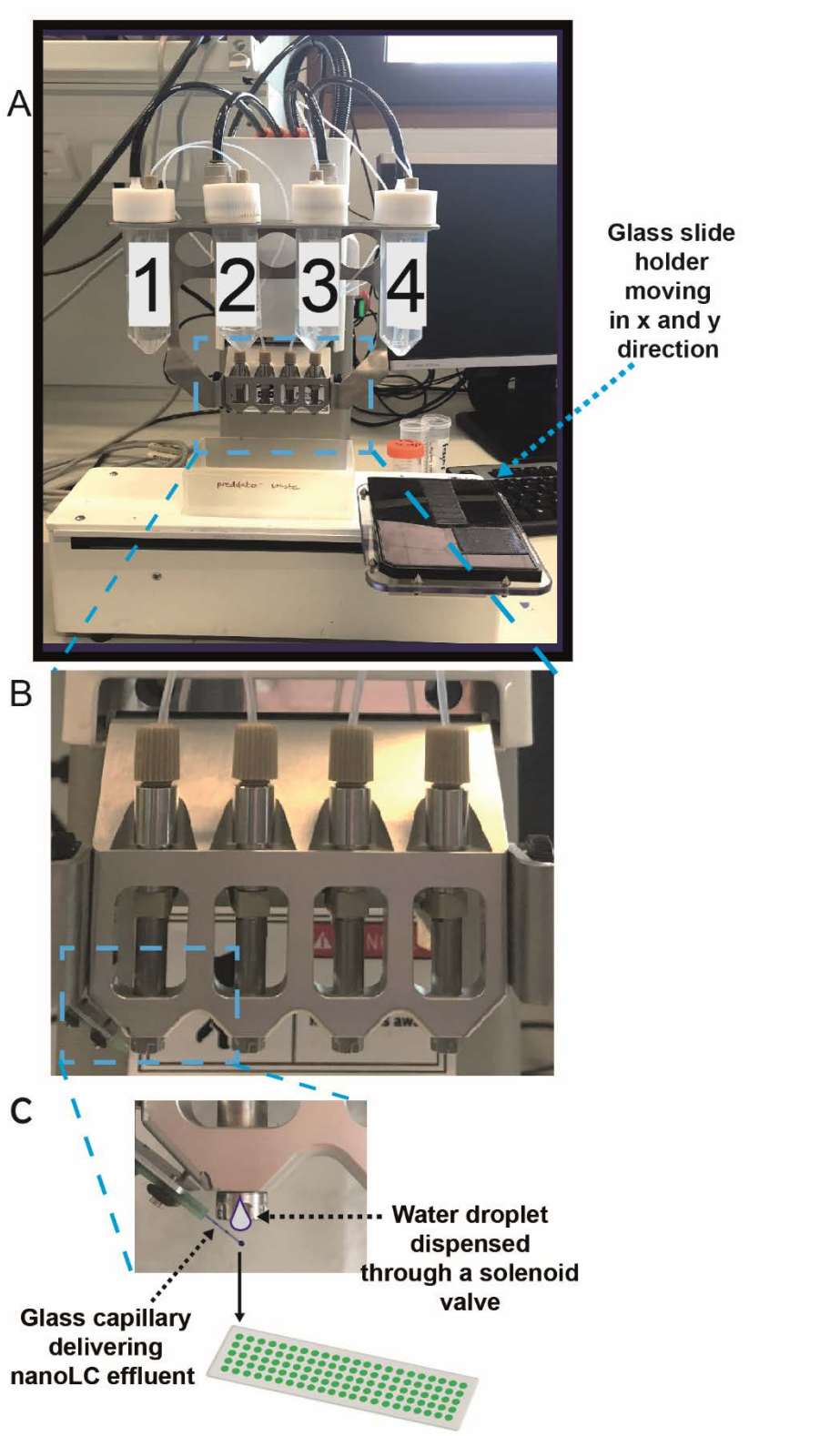

Figure S2. A: a low volume dispenser consisting of 4 pressurized containers (1-4) which are used to dispense different solutions; B: 4 solenoid valves; C: the most left positioned solenoid valve was used to dispense water droplets facilitating the dispensing of nanoLC effluent on the glass slide.

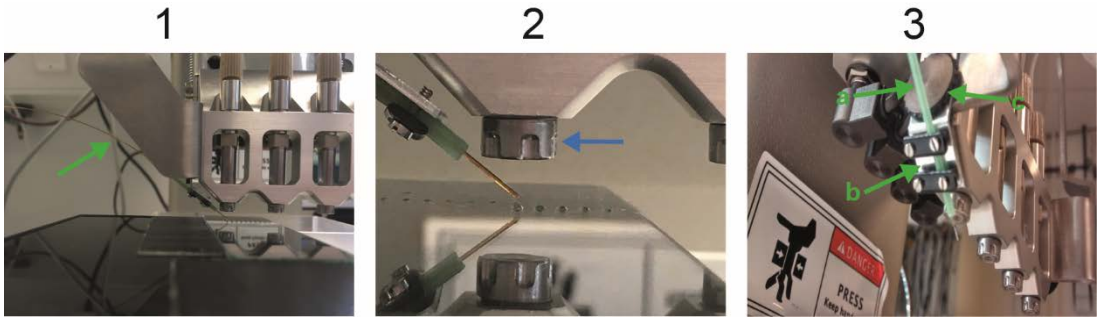

Figure S3. Coupling of nanoLC with the low volume dispenser. 1) Interface of nanoLC capillary (indicated with a green arrow) with the arm of the liquid dispenser; 2) Positioning of the capillary tip showing the angle of the capillary in relation to the spotter nozzle (nozzle indicated with a blue arrow); 3) Capillary holder in which a fluorinated ethylene polypropylene (FEP) tubing sleeve (a) is shown from the bottom of the liquid dispenser arm; the holder comprises two straps made of polyamide type 6.6 fitted with four screws (b) holding the nanoLC capillary positioned in the FEP tubing sleeve; (c) indicates a screw by which the capillary holder is connected to the arm of the liquid dispenser.

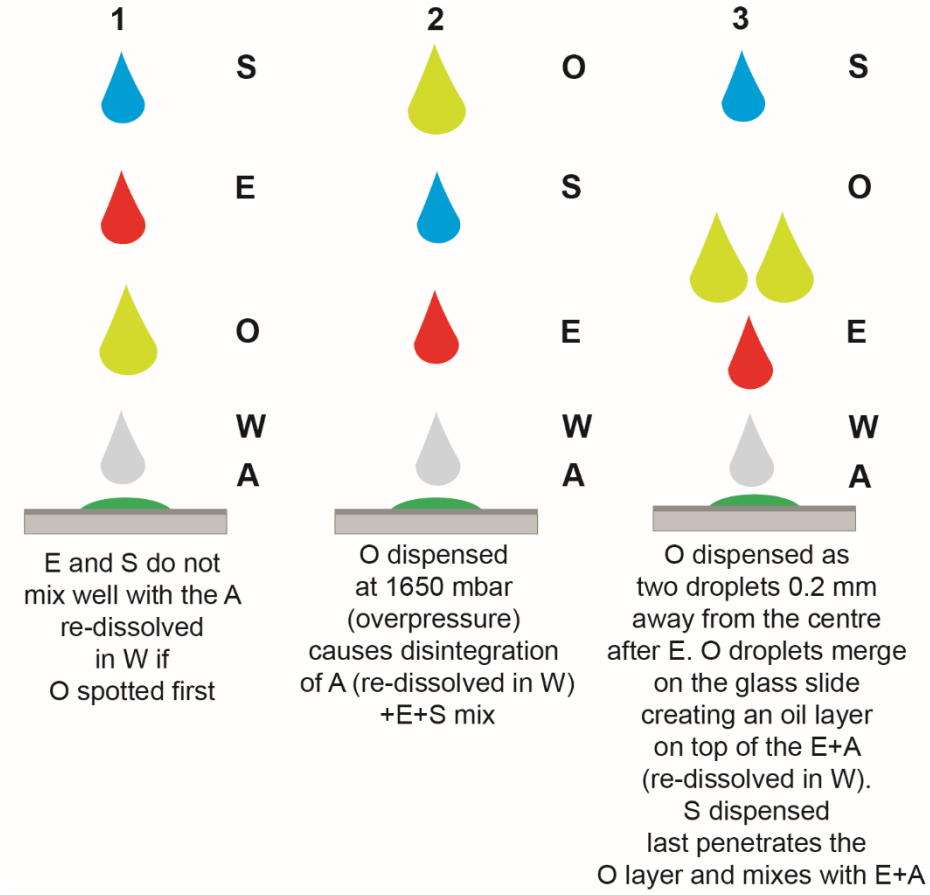

Figure S4. Different approaches tested for covering the microarray bioassay with mineral oil to prevent evaporation. 1) Mineral oil (O) spotted first on the deposited analyte (A) that was redissolved in water (W); 2) Mineral oil spotted last on the enzyme (E) + substrate (S) + A redissolved in W spot mix causing its disintegration; 3) Mineral oil spotted as two droplets 0.2 mm away from the center of the E droplet (one to the left and the other to the right side), followed by dispensing S.

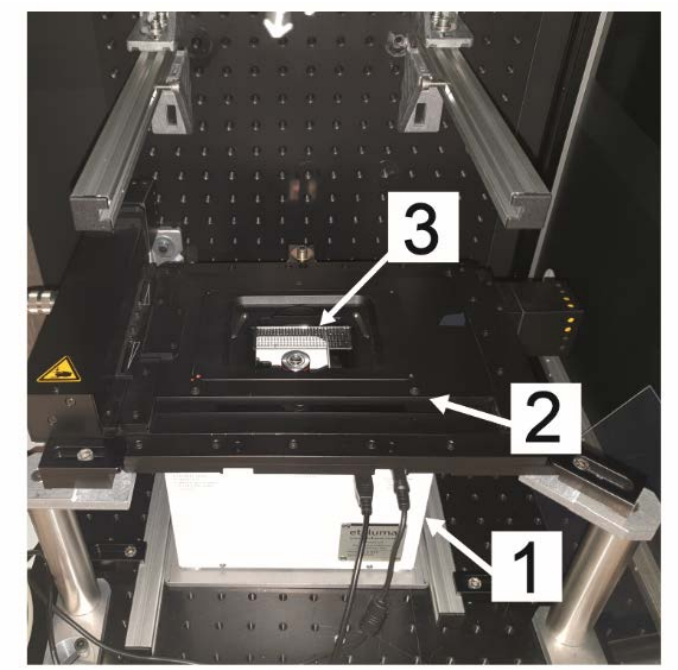

Figure S5. 1) Lumascope inverted fluorescence microscope with 2) a Märzhäuser high accuracy X,Y-stage fitted on top. In order to position the XY stage, the deck cover of the Lumascope was removed. The fluorescence microscope was equipped with 405, 488 and 590 nm light emitting diodes (LEDs), and a set of five Semrock filters, i.e. three excitation filters, a triple bandpass dichroic filter and a triple bandpass emission filter. For image capturing a digital camera containing a high sensitivity monochrome CMOS sensor was used; for focusing 3) an infinity corrected microscope objective (4x magnification; numerical aperture (NA) 0.13, working distance (WD) 17.2 mm, type number MA1012 from Meiji Techno) was placed in the objective holder of the Lumascope (the camera objective is changeable in Lumascope).

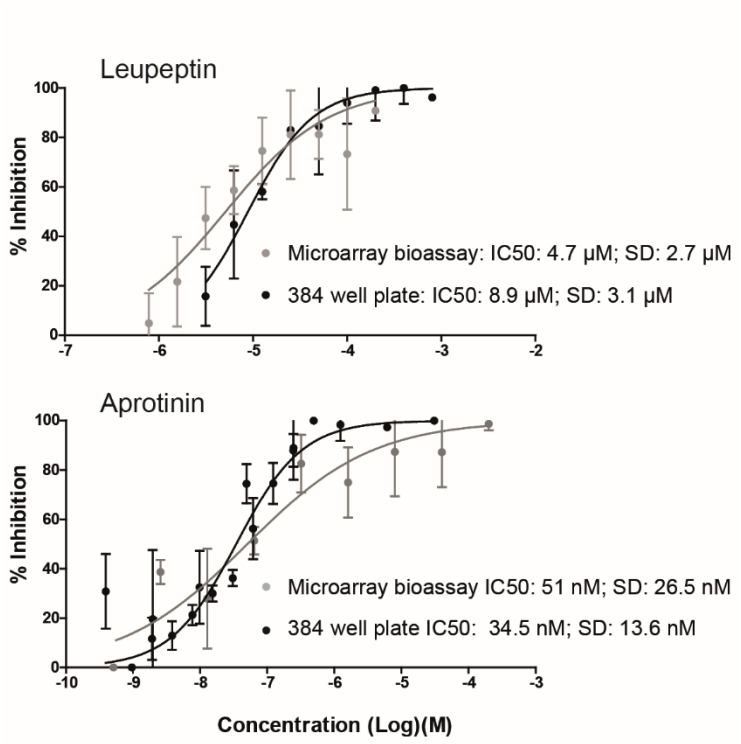

Figure S6. Comparison of IC50 curves of 1) leupeptin and 2) aprotinin obtained by the microarray bioassay (grey curves) with data obtained from a standard 384-well platereader assay format (black curves). To generate microarray bioassay IC50 curves, 100 nanoliter droplets of the inhibitors at different concentrations (the droplets dried rapidly after deposition) were collected on an MTMOS coated glass slide with the help of a syringe infusion pump that mimicked the nanoLC solvent delivery and maintained a continuous flow of the inhibitor solutions prior to microarray bioassay preparation.

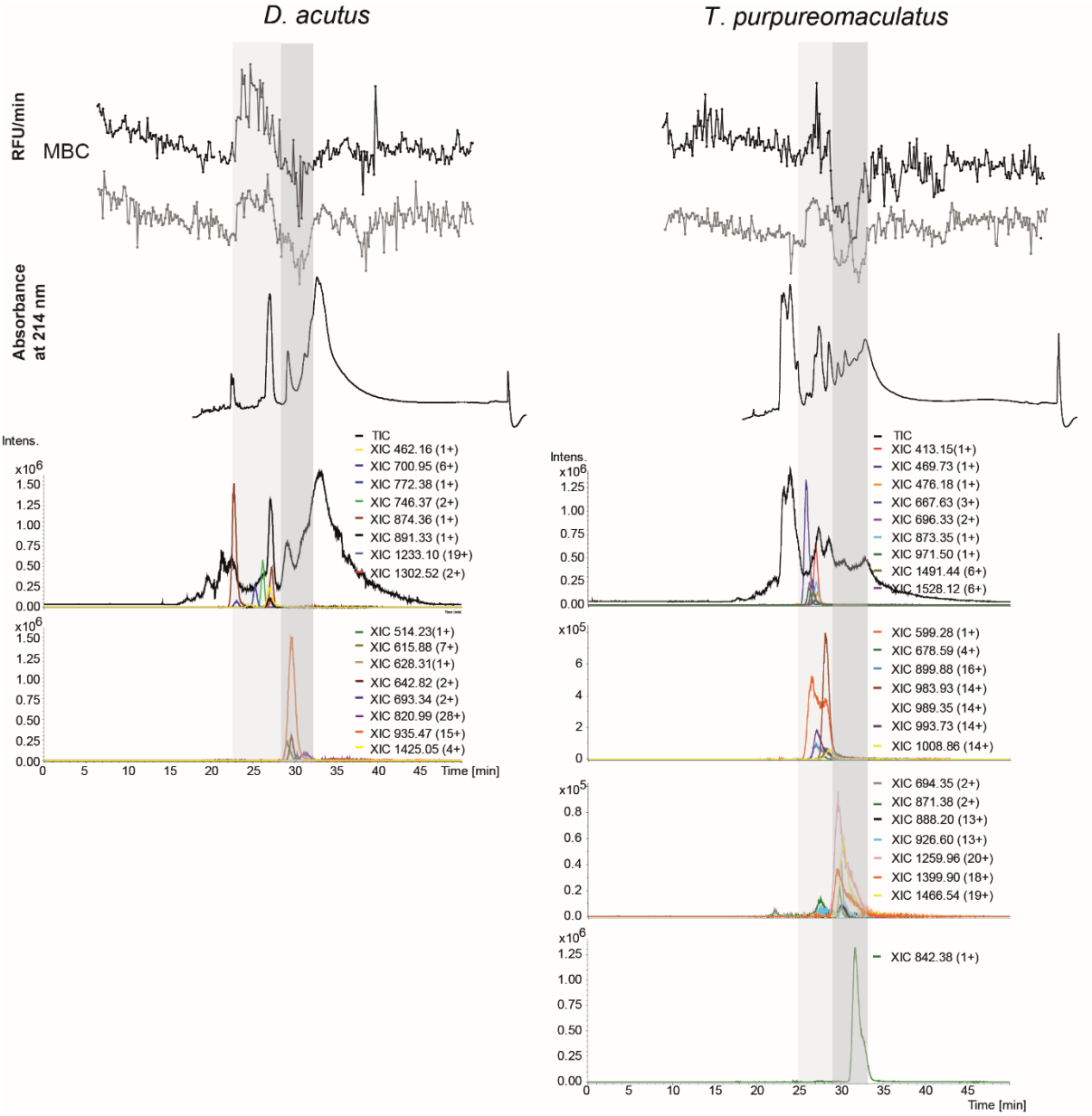

Figure S7. Picofractionation with microarray bioactivity profiling (i.e. plasmin inhibition and protease activity) of venoms of *D. acutus* and *T. purpureomaculatus.* The *D. acutus* results show two types of bioactivity: a positive (at 23-28 min) indicates the potential presence of proteases and/or fibrinolytic compounds, and a negative (at 28-32 min) that could indicate antifibrinolytic activities. From the parallel-obtained MS data, multiple masses are found to match the positive and negative peak areas of the microarray bioactivity chromatograms (MBCs) as shown as XICs. The MBC of *T. purpureomaculatus* also shows a positive peak(s) (at 25-29 min) and negative bioactivity peak(s) (at 29-33 min). The width of the positive and of the negative bioactive peak indicates the presence of multiple bioactive peptides or proteins.

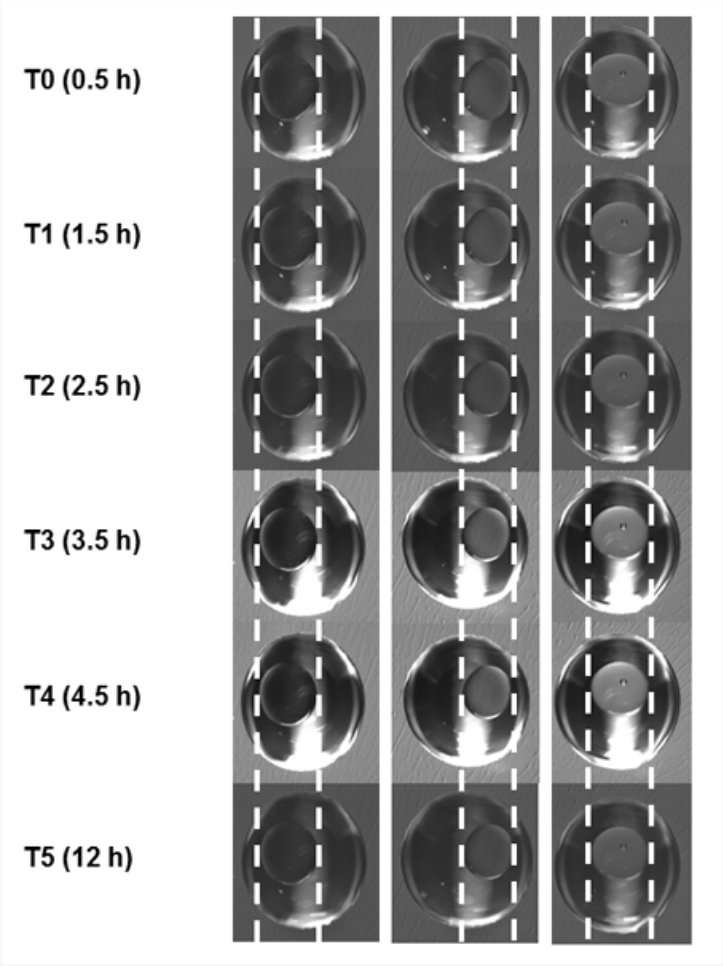

Figure S8. Three bioassay droplets were monitored for approximately 12 hours. The droplets consisted of a mixture of 100 nL enzyme and 100 nL substrate, and two mineral oil droplets of 200 nL each on top.

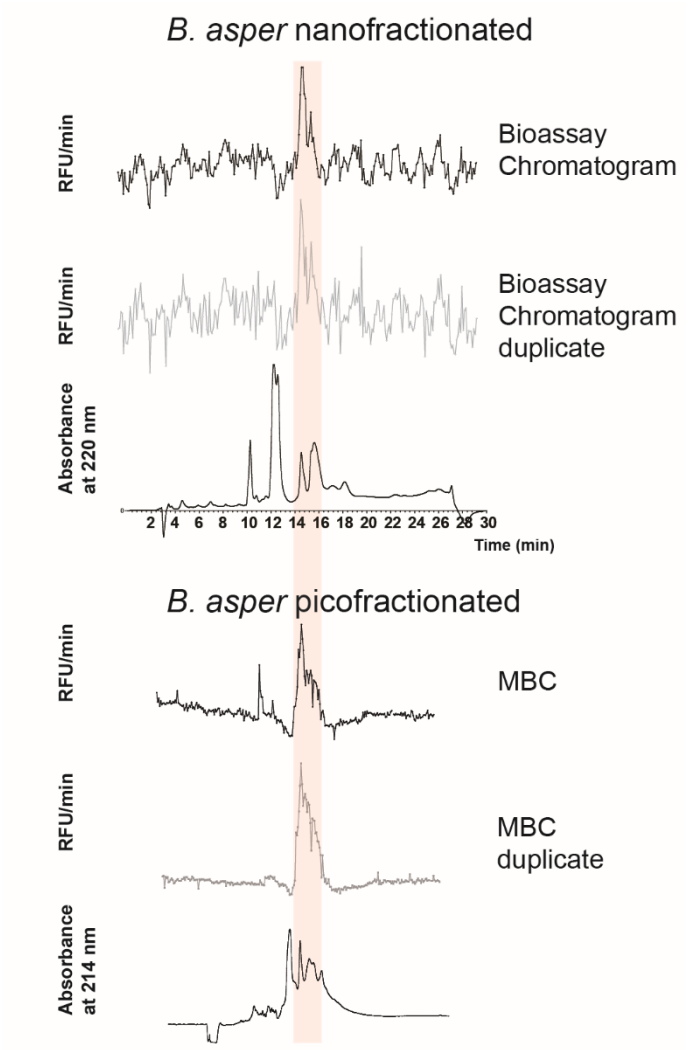

Figure S9. Top: Bioassay chromatograms of *B. asper* venom correlated to UV at 220 nm. The reanalysis of the venom was performed with a nanofractionation system. 6-s fractions of the venom (injected concentration 4 mg/mL) were collected on a 384 microtiter well plate, and after drying, exposed to a plasmin bioassay. Bottom: Data obtained from the measurements of *B. asper* with the picofractionation system (results provided as Figure 5 in the main document). MBC = microarray bioassay chromatogram; RFU/min = relative fluorescence unit/min.

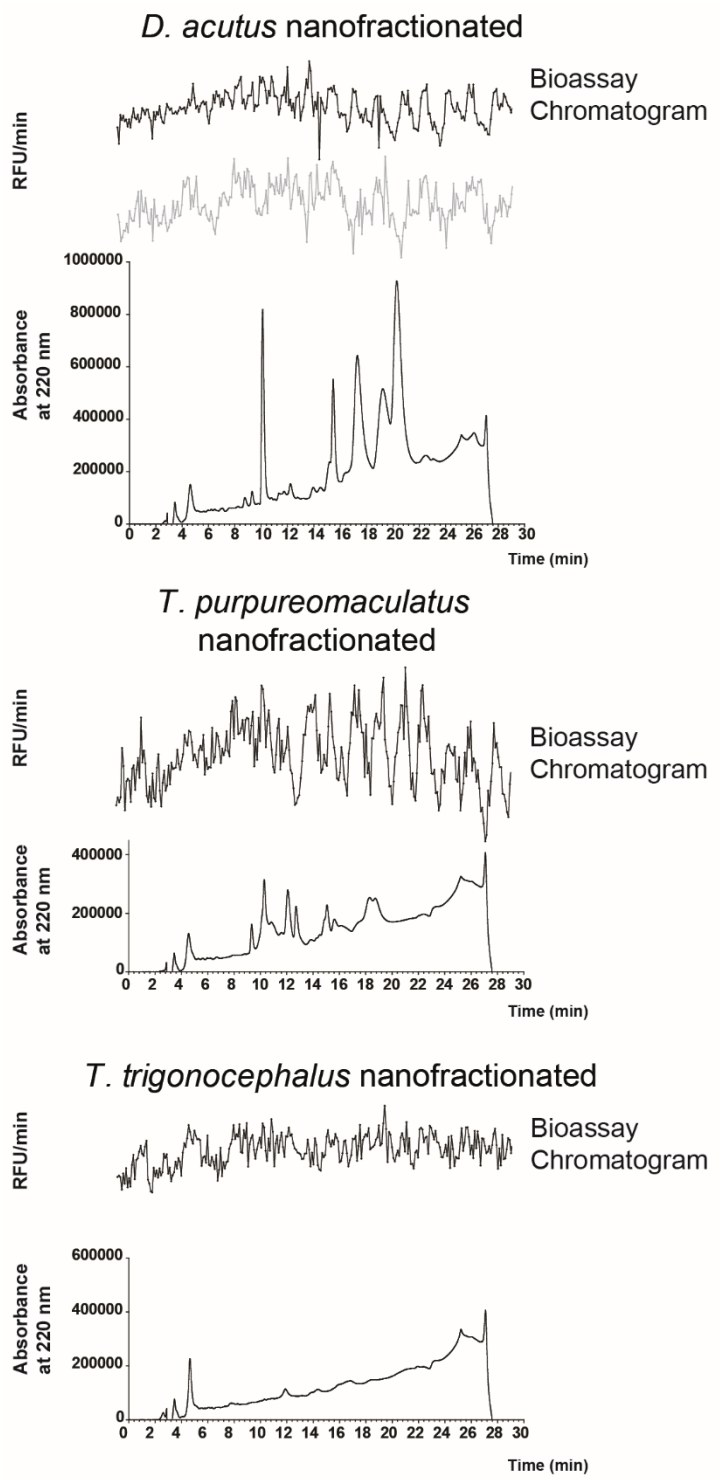

Figure S10. Bioassay chromatograms of *D. acutus*, *T. trigonocephalus* and *T. purpureomaculatus* correlated to UV at 220 nm. The reanalysis of the venoms was performed with a nanofractionation system. 6-s fractions of the venoms (injected concentration 4 mg/mL) were collected on a 384 microtiter well plate, and after drying, exposed to a plasmin bioassay. Detailed information on the measurement and description of the obtained data can be found in the Supporting Information section S10. RFU/min = relative fluorescence unit/min.

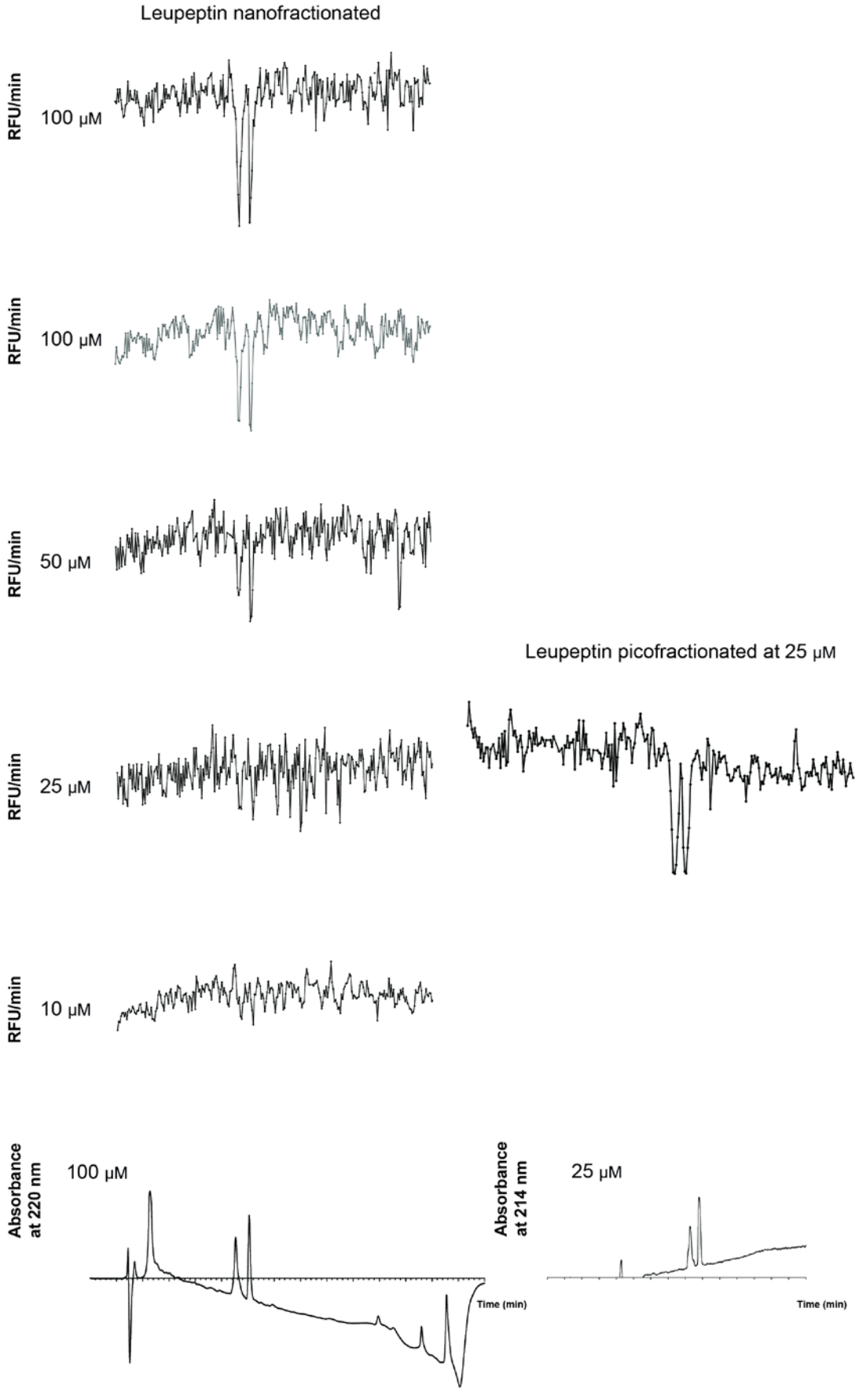
Leupeptin nanofractionated
RFU/min
100 µM
RFU/min
100 µM
RFU/min
50 µM
Leupeptin picofractionated at 25 µM
RFU/min
25 µM
RFU/min
10 µM
Absorbance at 220 nm
100 µM
Time (min)
Absorbance at 214 nm
25 µM
Time (min)

Figure S11. Superimposed bioactivity chromatograms resulting from bioassays of nanofractionated leupeptin standards injected at different concentrations on normal-bore LC-UV. All bioactivity chromatograms were normalized. The bioactivity chromatograms are correlated with the LC-UV trace (bottom) obtained from measurement of leupeptin at 100 µM. The data show that the nanofractionation and picofractionation platforms provide comparable results. RFU/min = relative fluorescence unit/min. Note that the separation efficiency between the leupeptin serial dilution in nanofractionation and picofractionation is not similar as a fast 30 minute gradient was used for the picofractionation serial dilution experiments (Figure 3 in the manuscript). For better comparison of resolution and sensitivity, a picofractionation analysis of leupeptin at 25 µM concentration using the long 60 minute gradient is depicted on the right side of the figure. These results show an increased sensitivity of the picofractionation compared to nanofractionation, while maintaining the same resolution (i.e. baseline separation) as for leupeptin in the nanofractionation. With the 60 minute gradient (right side of this figure and Figure 4 in the main document), peaks were separated in a similar fashion as for nanofractionation.

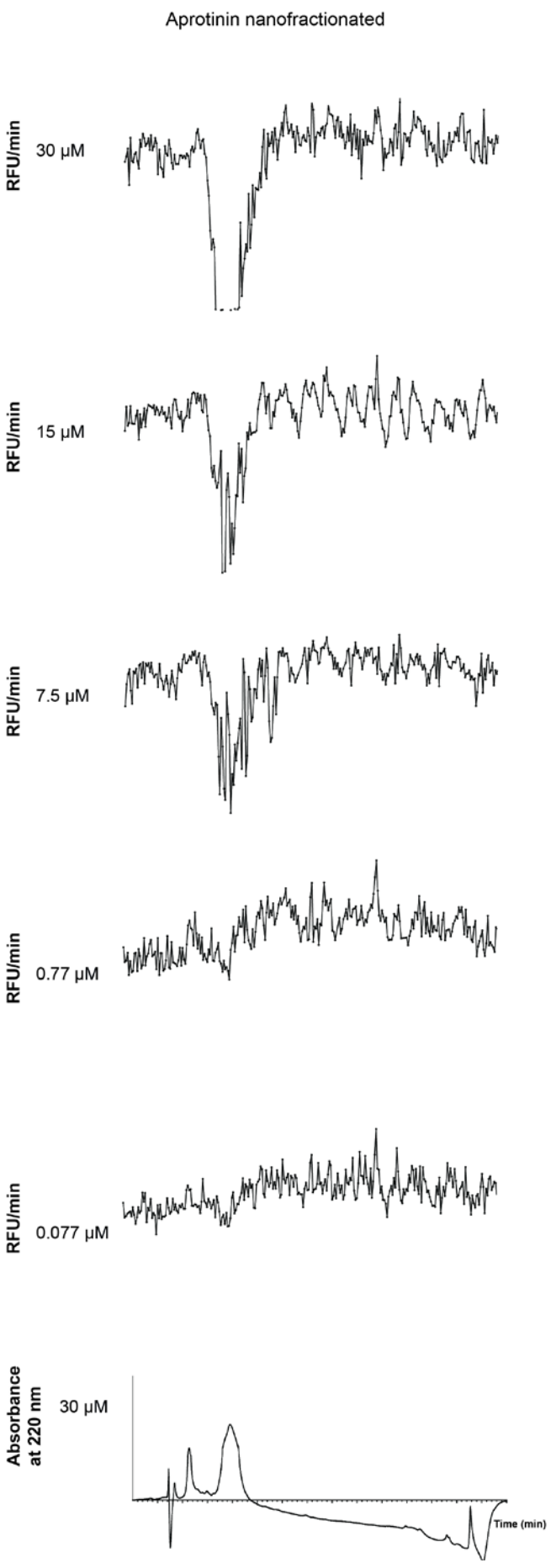
Aprotinin nanofractionated
RFU/min
30 µM
RFU/min
15 µM
RFU/min
7.5 µM
RFU/min
0.77 µM
RFU/min
0.077 µM
Absorbance at 220 nm
30 µM
Time (min)

Figure S12. Superimposed bioactivity chromatograms resulting from bioassays of nanofractionated aprotinin standards injected at different concentrations on normal-bore LC-UV. The bioactivity data have been normalized. The bioactivity chromatograms are correlated with LC-UV traces (bottom) obtained from measurement of aprotinin at 30 µM. The data show that the nanofractionation and picofractionation platforms provide comparable results. RFU/min = relative fluorescence unit/min.

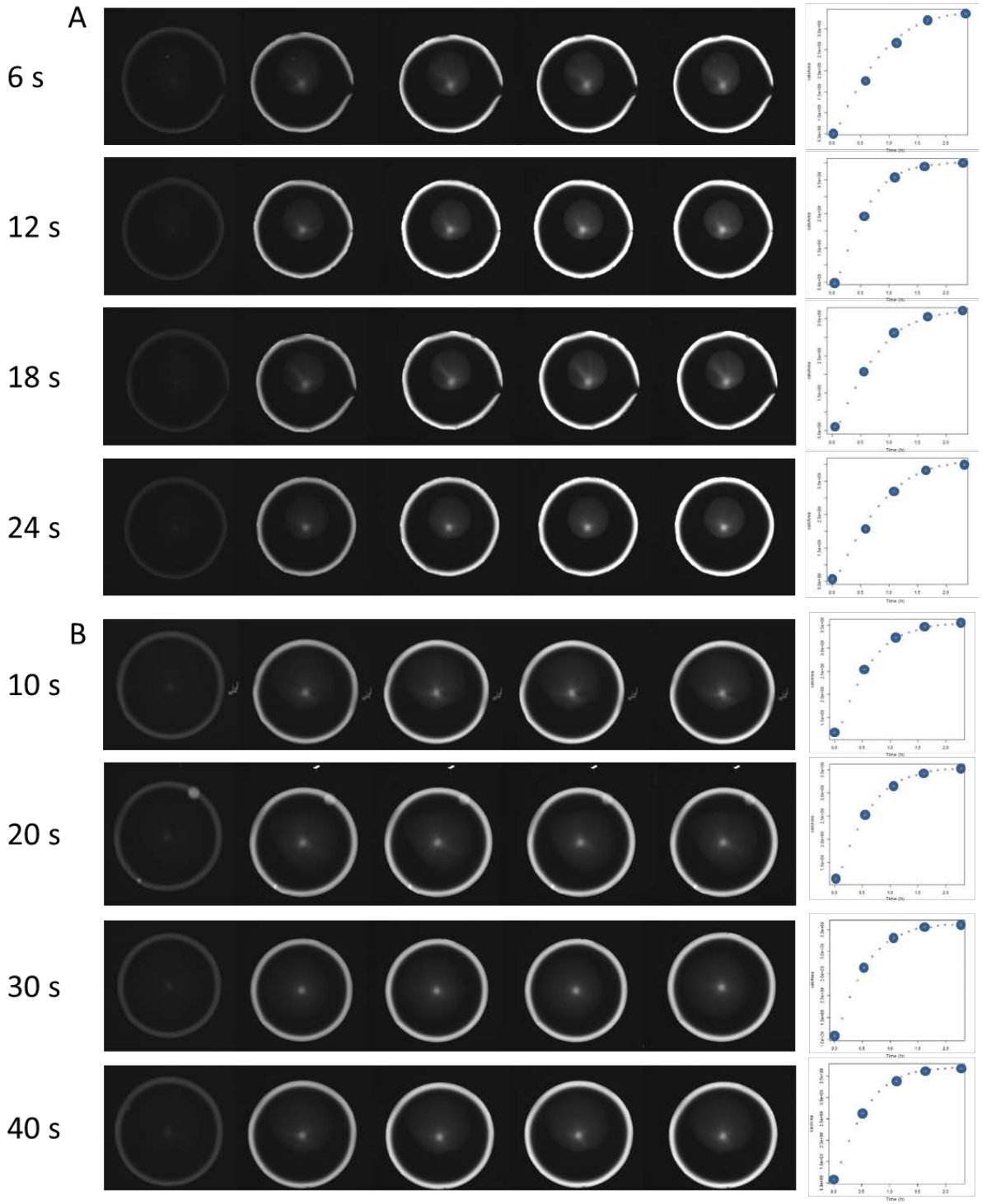

Figure S13. Comparison of the picofractionation frequency between 6- and 10-seconds. On the left side of the figure, a series of five pictures (individual droplets monitoring in time); on the right are kinetic curves obtained from the readout of the individual droplet monitored in time. All the droplets shown here were bioassayed according to the protocol described in "*Microarray plasmin-activity assay with fluorescence readout*". A) The kinetic curves of four spots are depicted after bioassay performance on 6-s fraction collected spots. Effective collection times of the four spots are 6, 12, 18 and 24 seconds, respectively. The full kinetic curve is obtained after taking 18 pictures in time as is described in Supporting Information S12. The five pictures (horizontal) represent readout 1, 5, 9, 13

and 18 of the kinetic curve, as is depicted by the dots in the graph to the right. This graph gives the kinetic curve of each individual spot. B) the kinetic curves of four spots are depicted after bioassay performance on 10-s fraction collected spots. Effective collection time of the four spots are 10, 20, 30 and 40 seconds, respectively. Figure S13B, shows five pictures. Again, picture 1, 5, 9, 13 and 18 as is depicted by the dots in the graph. As can be seen both spot monitoring and kinetic curve are very similar at both fractionation velocities.

Table S1. Mass-to-charge values (*m/z*) of small molecular ions, peptides and proteins that were found to elute at the retention time (t_R) corresponding to the bioactivity peaks. Mr, molecular mass.

T. purpureomaculatus				***T. trigonocephalus***				***B. asper***				***D. acutus***			
t_R (min)	***m/z***	***z***		**t_R (min)**	***m/z***	***z***	**Mr**	**t_R (min)**	***m/z***	***z***	**Mr**	**t_R (min)**	***m/z***	***z***	**Mr**
25-27	413.15	1	412.14	**22-25**	504.25	4	2012.97	**28-30**	946.41	15	14181.15	**23-28**	430.17	1	429.16
	426.18	1	425.17		546.28	2	1090.54		1032.95	14	14447.16		444.22	1	443.21
	430.17	1	429.16		550.24	1	549.23		984.78	14	13772.84		462.16	1	461.15
	444.19	1	443.18		594.80	1	593.79		935.47	15	14016.96		605.32	1	604.31
	469.73	1	469.72		619.83	1	618.81		527.23	1	526.22		653.33	1	652.32
	476.18	1	476.17		628.32	1	627.31		642.82	1	641.81		682.77	2	1363.52
	667.63	3	1999.88		635.85	1	634.84		706.84	1	705.83		700.95	6	4119.68
	696.33	2	1390.65		659.33	2	1315.64		822.57	17	13966.55		746.37	2	1490.73
	873.35	1	872.34		691.33	2	1380.64		820.81	17	13936.58		772.38	1	771.37
	953.49	1	952.48		723.36	2	1443.71	**31-33**	816.92	28	22845.5		859.34	1	859.33
	1528.12	6	9162.65		731.86	2	1461.71		852.32	28	23836.84		873.35	1	872.34
	971.50	1	970.49		738.86	2	1475.70		846.62	27	22831.45		874.36	1	873.35
	1491.44	6	8942.57		744.35	1	743.34		856.43	27	23096.58		891.33	1	891.32
	1068.55	1	1067.54		746.85	1	745.84		1269.46	23	29174.34		1049.24	5	5241.18
27-29	599.28	1	598.27		801.41	2	1600.8		1272.03	23	29233.51		1106.54	1	1105.53
	678.59	4	2710.33		872.41	1	871.40						1119.57	1	1118.56
	720.32	1	719.31		928.50	1	927.49						1156.48	1	1155.47
	941.67	15	14109.95		968.88	2	1935.75						1233.10	19	23364.66
	983.93	14	13760.89		987.99	2	1973.97						1288.50	1	1287.49
	923.40	15	13836.82	**25-28**	666.33	3	1995.97						1302.52	1	1301.51
	927.54	15	13898.09										1510.59	2	3019.17
29-31	694.35	2	1386.65		531.22	1	530.21						1718.67	1	1717.66
	871.38	2	1740.71		628.64	3	1882.88						1933.25	2	3864.49
	878.27	13	11404.45		797.71	3	2390.15								
	888.20	13	11533.46		801.88	2	1601.74					**28-32**	514.23	1	513.22

	926.60	13	12032.72		836.88	2	1671.74				615.88	7	4304.10
	1259.96	20	25179.17		906.84	2	1811.67				628.31	7	4391.14
	1466.54	19	27845.22		980.38	2	1958.75				642.82	2	1283.62
31-33	842.38	1	841.37		1043.93	2	2085.84				693.34	2	1384.66
					1053.69	4	4210.72				736.21	1	735.20
	989.32	14	13836.81		1098.43	8	9779.38				820.99	28	22959.52
	899.88	16	14382.03		1104.46	4	4413.8				1425.05	4	5696.19
	993.73	14	13898.06		1121.44	8	8963.4811						
					1152.96	8	9214.64						
					1162.21	8	9289.66						
					1313.66	18	23627.83						
					1295.09	7	9058.56						
					1350.18	18	24285.18						